Combinational Optoelectronic Circuit Based on SiC Technology

M.A. Vieira, M. Vieira, P. Louro, V. Silva, A. Fantoni
DEETC/. ISEL
Lisbon, Portugal
e-mail: mv@isel.ipl.pt

M.A. Vieira ,M. Vieira P. Louro, V. Silva, A. Fantoni
CTS/. UNINOVA
Monte de Caparica, Portugal
e-mail: mv@isel.ipl.pt

Abstract— **The purpose of this paper is the design of simple combinational optoelectronic circuit based on SiC technology, able to act simultaneously as a 4-bit binary encoder or a binary decoder in a 4-to-16 line configurations. The 4-bit binary encoder takes all the data inputs, one by one, and converts them to a single encoded output. The binary decoder decodes a binary input pattern to a decimal output code. The optoelectronic circuit is realized using a a-SiC:H double pin/pin photodetector with two front and back optical gates activated trough steady state violet background. Four red, green, blue and violet input channels impinge on the device at different bit sequences allowing 16 possible inputs. The device selects, through the violet background, one of the sixteen possible input logic signals and sends it to the output. Results show that the device acts as a reconfigurable active filter and allows optical switching and optoelectronic logic functions development. A relationship between the optical inputs and the corresponding digital output levels is established. A binary color weighted code that takes into account the specific weights assigned to each bit position establish the optoelectronic functions. A truth table of an encoder that performs 16-to-1 multiplexer (MUX) function is presented.**

Keywords- SiC Optoelectronic device, photonics, optical communications, MUX/DEMUX; encoders, logic functions.

I. INTRODUCTION

There has been much research on semiconductor devices as elements for optical communication, when a band or frequency needs to be filtered from a wider range of mixed signals or when optical active filter are used to select and filter input signals to specific output ports in WDM communication systems [1, 2].

Optical communication in the visible spectrum usually interfaces with an optoelectric device for further signal processing. Multilayered structures based on amorphous silicon technology are expected to become reconfigurable to perform WDM optoelectronic logic functions [3, 4]. They will be a solution in WDM technique for information transmission and decoding in the visible range [5]. The basic operating principle is the exploitation of the physical properties of a nonlinear element to perform a logic function, with the potential to be rapidly biasing tuned Any change in any of these factors will result in filter readjustments. Here, signal variations with and without front and back backgrounds move electric field action up and down in a known time frame. A truth table support new optoelectronic logic architecture.

II. DEVICE OPERATION

The optoelectronic circuit consists of a p-i'(a-SiC:H)-n/p-i(a-Si:H)-n heterostructure with low conductivity doped layers as displayed in Fig.1. The optoelectronic characterization was described elsewhere [6]. Monochromatic pulsed lights, separately (λ_R=626 nm, λ_G=526 nm, λ_B=470 nm, λ_V=400 nm; input channels) or in a polychromatic mixture (multiplexed signal) at different bit rates illuminated the device.

Independent tuning of each channel is performed by steady state violet optical bias (λ_{bias}= 2300 μW/cm^2) superimposed either from the front and back sides and the generated photocurrent measured at -8V. The device operates within the visible range using as input color channels (data) the wave square modulated light (external regulation of frequency and intensity) supplied by a red (R; 25 μW/cm^2), a green (G; 46 μW/cm^2), a blue (B; 40 μW/cm^2) and violet (V; 150 μW/cm^2) LED's.

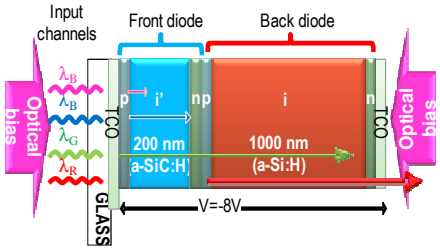

Figure 1. .Device configuration and operation.

III. OPTICAL BIAS CONTROLLED FILTERS

In Fig.2, the spectral photocurrent, normalized to its value without background is displayed, under front (a) and

 ISBN: 978-1-61208-297-4

back (b) violet irradiations and different intensities.

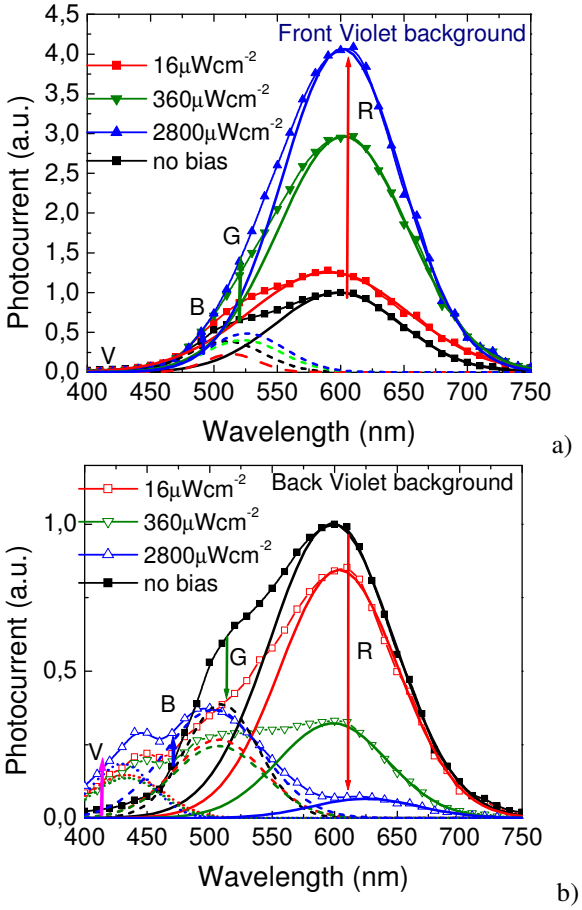

Figure 2. Normalized spectral photocurrent under front (a) and back (b) violet irradiations with different intensities.

A peak fit adjustment to the data was performed (lines) with peaks centered on 630 nm (solid), 520 nm (dash) and 430 nm (dot). Results show that under front violet irradiation, as the background intensity increases, the peak centered at 630 nm (red range) strongly increases while under back light an opposite behavior is observed and the red peak is strongly reduced (see arrows). Under front and back side irradiation, the peak at 520 nm (green range) increases slightly with the intensity. Under back irradiation, a new peak centered at 430 nm appears and increases with the background intensity. So, under front illumination the reddish part of the spectrum is strongly enhanced with the intensity while under back illumination the main enhancement occurs at the violet-blue region. A trade-off between the background intensity and the enhancement or quenching of the different spectral regions, under front and back irradiation, has to be established.

In Fig. 3 the spectral gain (α^V), defined as the ratio between the spectral photocurrents under violet illumination (applied from the front and back sides) and without it, is plotted at 3500 Hz and 2300μWcm^{-2}. As expected from Fig. 2, under back bias the gain is high at short wavelengths and strongly lowers for wavelengths higher than 500 nm, acting as a short-pass filter. Under violet front light the device works as a long-pass filter for wavelengths higher than 550 nm, blocking the shorter wavelengths. Results show that by combining the background wavelengths and the irradiation side the short-, and long- spectral region can be sequentially tuned. The medium region can only be tuned by using both active filters.

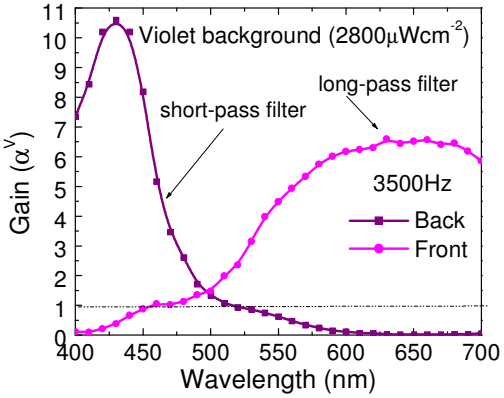

Figure 3. Spectral gain under violet (αV) optical bias, applied from the front and the back sides at 3500Hz.

IV. ENCODER AND DECODER DEVICE

A. *Optical switching*

Four monochromatic pulsed lights separately (red, green, blue and violet input channels, Fig. 4) or combined (multiplexed signal, Fig. 5) illuminated the device at 12000 bps. Steady state violet optical bias was superimposed separately from the front (a) and the back (b) sides and the photocurrent measured. In Fig. 4, the transient signals were normalized to their values without background and added the mean values of the optical gains for each individual channel.

Results show that, even under transient conditions and using commercial LED's as pulsed light sources, the background side affects the signal magnitude of the color channels. As in Fig. 2, under front irradiation, it enhances mainly the spectral sensitivity in the medium-long wavelength ranges (α^V_R=4.7, α^V_G=2.4). Violet radiation is absorbed at the top of the front diode, increasing the electric field at the back diode [7] where the red and part of the green incoming photons are absorbed (see Fig. 1). Under back irradiation the electric field increases mainly near the front p-n interface where the violet and part of the blue incoming channels generate most of the photocarriers (α^V_V=11, α^V_B=1.5). So, by switching between fronts to back irradiation the photonic function is modified from a long- to a short-pass filter allowing, alternately selecting the red or the violet channels.

 ISBN: 978-1-61208-297-4

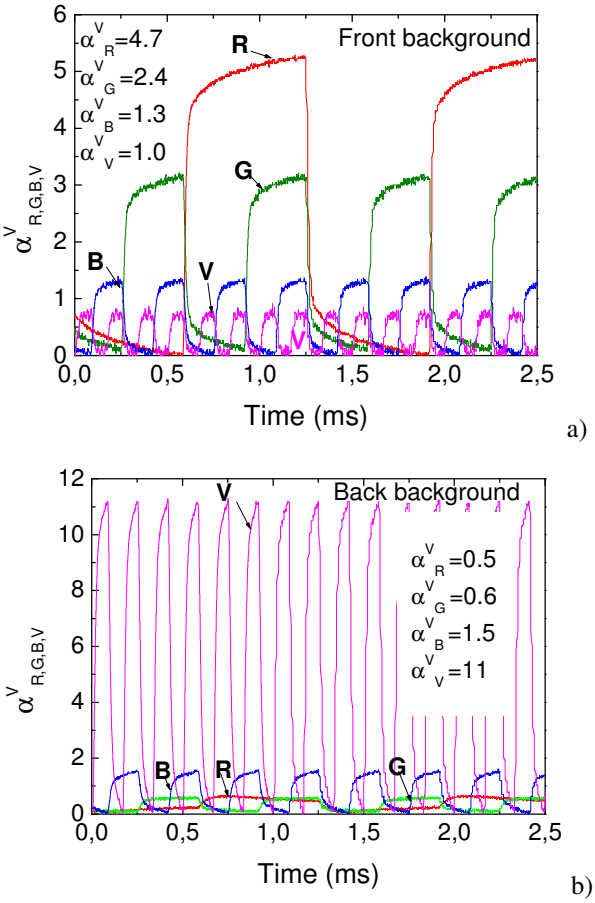

Figure 4. Normalized red (R), green (G) blue (B)and violet (V) transient signals at -8V with violet (400 nm) steady state optical bias applied from the front (a) and from the back (b) sides.

B. *Optoelectronic logic functions*

For an optoelectronic digital capture system, opto-electronic conversion is the relationship between the optical inputs and the corresponding digital output levels.

Fig. 5 displays the normalized MUX signals due to the combination of the input channels of Fig. 4, without and under front (a) and back (b) violet irradiations. On the top the signals used to drive the input channels are displayed showing the presence of all the possible 2^4 *on/off* states. For comparison the MUX signal without optical bias is displayed (dark) in both figures.

Results show that the side of background affects the form and the magnitude of the MUX signal in opposite ways. Under front irradiation, sixteen levels (2^4) are detected and grouped into two main classes due to the high amplification of the red channel (α^V_R>>1; Fig. 4a). The upper eight (2^3) levels are ascribed to the presence of the red channel (R=1), and the lower eight to its absence (R=0), allowing the red channel decoder (8-to-1 multiplexer; long-pass filter function). Since under front irradiation the green channel is also amplified,(α^V_G>1) the four highest levels, in both classes, are ascribed to the presence of the green channel (G=1) and the four lower ones to its lack (G=0).

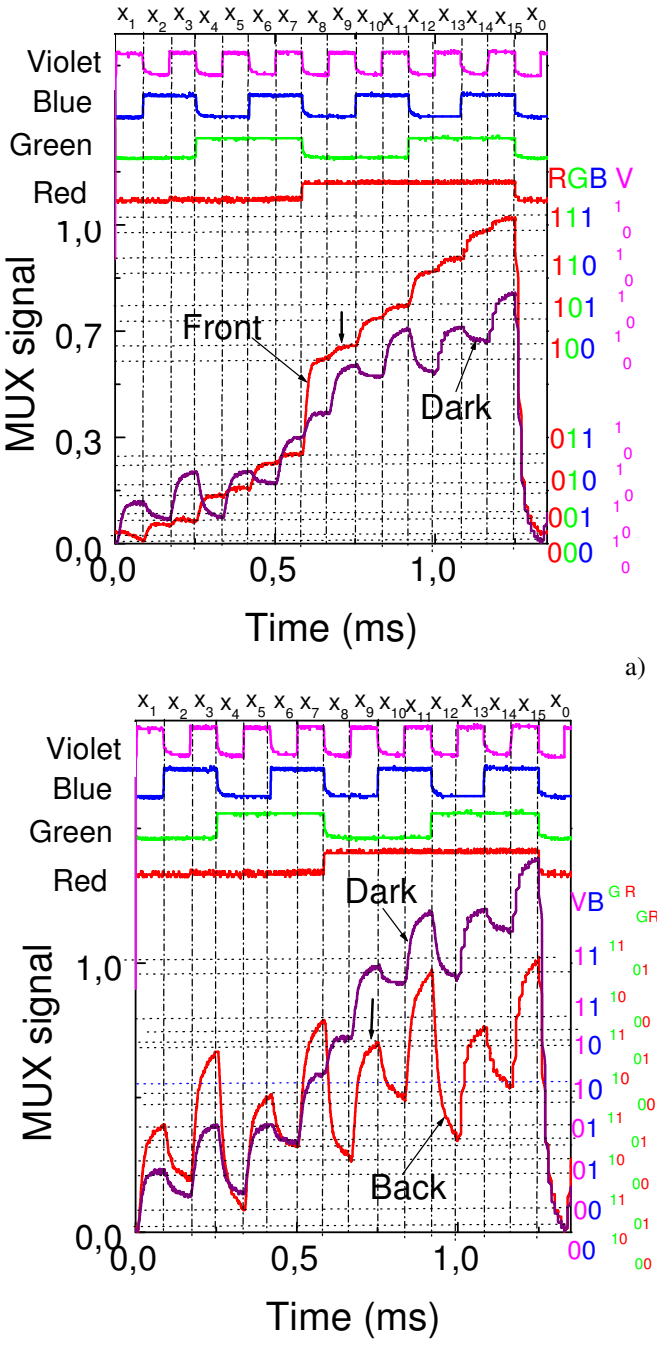

Figure 5. Normalized multiplexed signal under front (a) and back (b) violet irradiation and without it (dark). On the top the signals used to drive the input channels are shown to guide the eyes into the ON/OFF channel states.

The blue channel is slightly amplified, so, in each group of 4 entries, two levels (2^1) can be found: the two higher levels correspond to the presence of the blue channel (B=1) and the two lowers to its absence (B=0). Finally, each group of 2 entries have two near sublevels, the higher where the

 ISBN: 978-1-61208-297-4

violet channels is ON (V=1) and the lower where it is missing (V=0). Under back irradiation, the violet channel is strongly enhanced, the blue channel is slightly and the green and red reduced (α^{V}_{R} and $\alpha^{V}_{G}<1$ and $\alpha^{V}_{B}>1$ and $\alpha^{V}_{V}>>1$; Fig. 4b). The encoded multiplexed signal is, also, made of sixteen sublevels grouped into two main levels, the higher where the violet channel is ON (V=1) and the lower where it is OFF (V=0) (8-to-1 multiplexer; short-pass filter function). Each group the eight sublevels can be grouped in two classes, with and without the blue channel ON. Each of those classes split into four near sublevels, attributed to the presence or absence of the red and green channel. If we consider this red and green output bits "not significant" only four separate levels (2^2) are considered and the logic MUX function is converted into a logic filter function. The violet channel is then decoded.

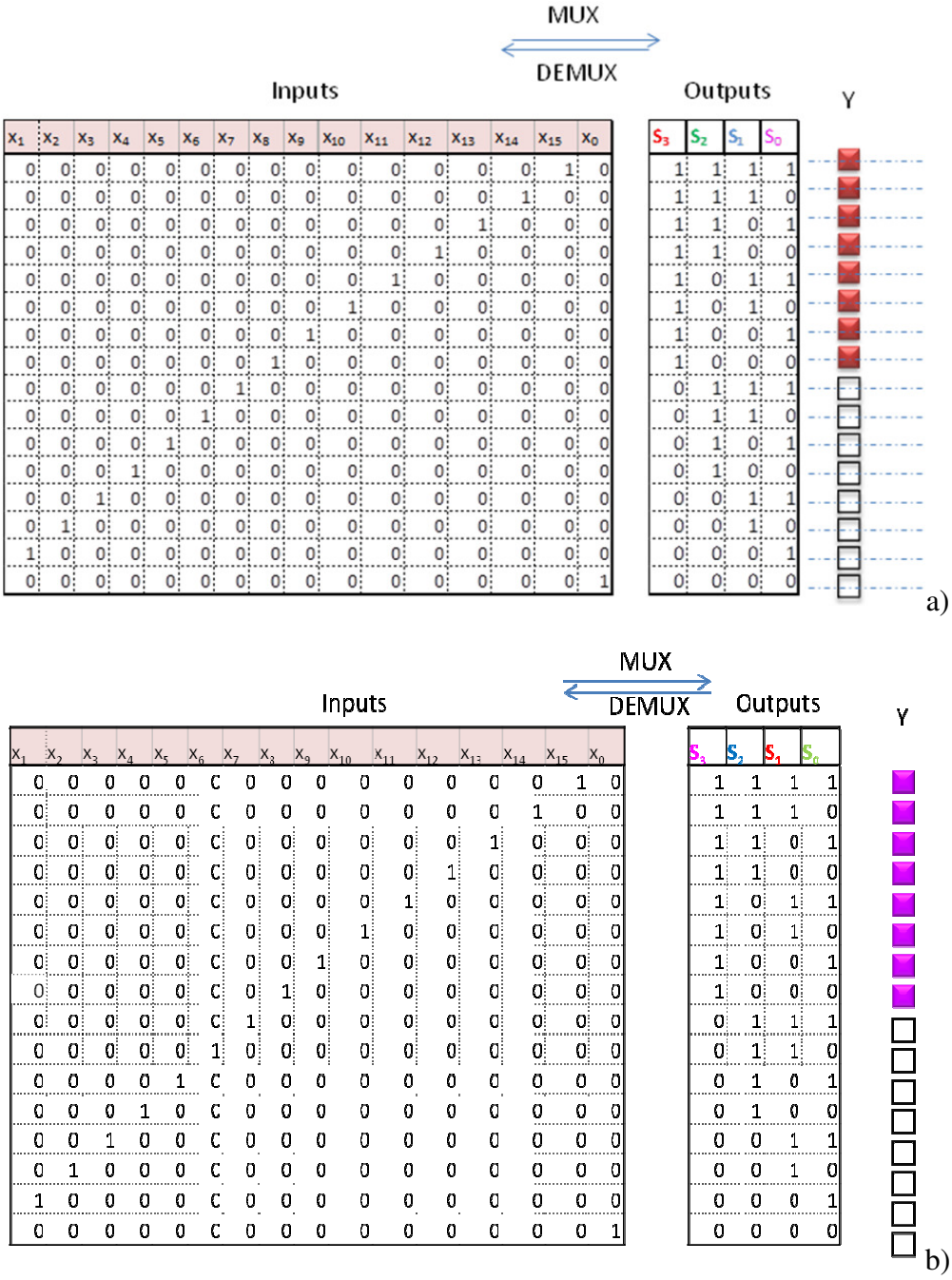

Figure 6. Truth table of the encoders that perform 16-to-1 multiplexer (MUX) function, under front (a) and back (b) violet irradiations.

The binary code is an arithmetic code and so, it is weighted, *i. e*. there is specific weights assigned to each bit position. Due to the different optical gains (Fig. 3), the selection index for those 16-element look-up table are a 4-bit binary [RGBV] code under front irradiation or a 4-bit binary [VBGR] of the form [S_3, S_2, S_1,S_0] where S_n means the color channel (right side of Fig. 5) with n weighted by the amplification factor (Fig. 4). The multiplexer select code represents an address or index, into the ordered inputs.

The truth tables of the encoders of Fig. 5, that perform 16-to-1 MUX function, are shown in Fig. 6. The correspondence between the on/off state of the input channels and the [RGBV] code under front irradiation, and the [VBRG] code under back irradiation are obvious. In the inputs (x_0….x_{15}), the index of each bit, is related to the first (highest) nonzero logic input. Here, the MUX device selects, through the front or back violet backgrounds, one of the sixteen possible input logic signals and sends it to the output ($y=x_S$). In Fig. 6a the output is a 4-bit binary RGBV number that may identify one of sixteen possible inputs. Just as the multiplexer has a binary code for the selection of an input, the demultiplexer (DEMUX) has a similar code for selecting a particular output. The 4-bit output RGBV code allows designing an encoder to transform a four-line-to-sixteen-line decoder. From truth table of Fig. 6a, the Boolean functions for the encoder with inputs x_0 to x_{15} and outputs R, G, B, V is given as:

$$R(S_3)=\sum(8,9,10,11,12,13,14,15);$$
$$G(S_2)=\sum(4,5,6,7,12,13,14,15);$$
$$B(S_1)=\sum(2,3,6,7,10,11,14,15);$$
$$V(S_0)=\sum(1,3,5,7,9,11,13,15).$$

A binary representation for decimal number 9 is in RGBV code "1001" ($2^3+0+0+2^0$) under front irradiation and it corresponds to both red and violet channels ON. Under back irradiation (VBRG code) the binary representation is the same although the weights assigned to each bit position are different (see arrows in Fig. 5). This 4-bit output RGBV code allows us design a 4-to-10 line decoder to transform a decimal number (0 to 9) into a binary code. The 4-bit codes from 1010 through 1111 do not arise from the encoding of the decimal numbers.

V. DATA ROUTER

Whereas the multiplexer is a data selector, the demultiplexer is a data distributor or data router. Just as the multiplexer has a binary code (RGBV) for the selection of an input, the demultiplexer has a similar code for selecting a particular output. In the pi'n/pin device the side of the background is the routing control for the data source. The front and back background acts as selector to select one of the four incoming channels by splitting portions of the input multi-channel optical signal across the front and back photodiodes. This duality of functions is characteristic of decoders and demultiplexers.

Under front background the red channel is decoded due to its higher amplification while under back violet irradiation the violet channel is selected (Figs. 5 and 6). To help to decode the green and blue channels, in Fig. 7 the difference between the multiplex signal under front and back violet irradiation is displayed.

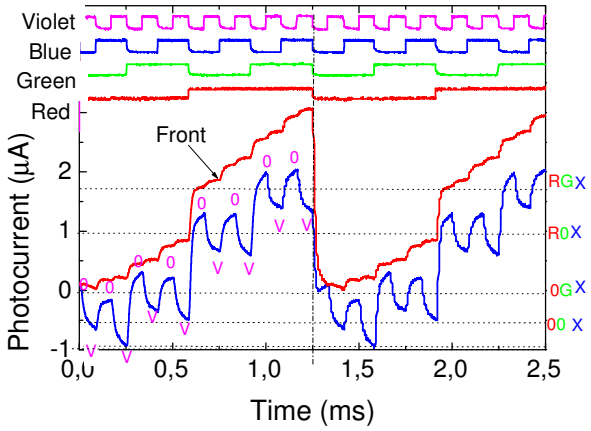

Figure 7. Wavelength difference generation. On the top the signal to drive the input channels guide the eyes.

This difference wavelength generation is a consequence of nonlinear interaction of the device with the front or back backgrounds and the optical channels generation. It weights the red versus violet content of the measured signal, so, it enhances the effect of the routing control and offers a transparent wavelength conversion. The presence of the red channel pushes the difference up and the violet channel pushes it down (right side of Fig. 5). The blue channel does not affect the difference. So, after decoding the red and the violet transmitted information and comparing with difference wavelength generation levels in the same time slots, the green and blue signals can be immediately decoded.

We have used this simple algorithm to perform 1 -to-16 demultiplexer (DEMUX) function and to decode the multiplex signals. As proof of concept the decoding algorithm was implemented in *Matlab* [8] and tested using different binary sequences. In Fig. 8a a random MUX signal under front and back irradiation is displayed and in Fig. 8b the decoding results are shown. On the top of both figures the signals to drive the LED's and the DEMUX signals obtained as well as the binary bit sequences are respectively displayed. A good agreement between the signals used to drive the LED's and the decoded sequences is achieved. In all sequences tested the RGBV signals were correctly decoded.

The DEMUX sends the input logic signal to one of its sixteen outputs, according to the optoelectronic demux algorithm. So, by means of optical control applied to the front or back diodes, the photonic function is modified, respectively from a long- pass filter to pick the red channel to a short-pass filter to select the violet channel, giving a step reconfiguration of the device. The green and blue channels are selected by combining both active long- and

 ISBN: 978-1-61208-297-4

short-pass filters into a band-pass filter. In practice, the decoding applications far outnumber those of demultiplexing. Multilayer SiC/Si optical technology can provide a smart solution to communication problem by providing a possibility of optical bypass for the transit traffic by dropping the fractional traffic that is needed at a particular point.

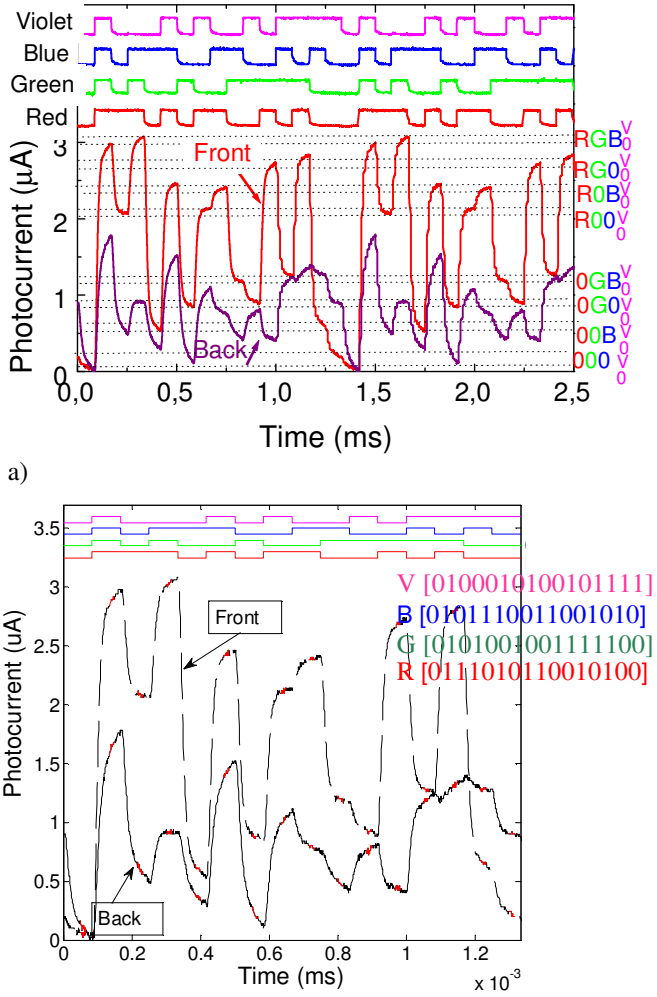

Figure 8. MUX signal under front and back irradiation. On the top a) Signals used to drive the LED's. b) DEMUX signals and decoded RGBV binary bit sequences.

VI. CONCLUSIONS

An optoelectronic device based on a-SiC:H technology is analyzed. The device is able to act simultaneously as a 4-bit binary encoder or a binary decoder in a 4-to-16 line configurations.

A relationship between the optical inputs and the corresponding digital output levels is established. A binary weighted color code that takes into account the specific weights assigned to each bit position establish the optoelectronic functions. A truth table of an encoder that performs 16-to-1 multiplexer (MUX) function is presented. A decode algorithm based on the optical bias control of the device was improved.

More work as to be done in order to execute optical arithmetic micro-operations entirely within the optical domain.

ACKNOWLEDGEMENTS

This work was supported by FCT (CTS multi annual funding) through the PIDDAC Program funds and PTDC/EEA-ELC/111854/2009 and PTDC/EEA-ELC/120539/2010.

REFERENCES

1. C. Petit, M. Blaser, Workshop on Optical Components for Broadband Communication , ed. by Pierre-Yves Fonjallaz, Thomas P. Pearsall, Proc. of SPIE Vol. 6350, 63500I, (2006).
2. S. Ibrahim, L. W. Luo, S. S. Djordjevic, C. B. Poitras, I. Zhou, N. K. Fontaine, B. Guan, Z. Ding, K. Okamoto, M. Lipson, and S. J. B. Yoo, paper OWJ5. Optical Fiber Communications Conference, OSA/OFC/NFOEC, San Diego, 21 Mar 2010.
3. M.A. Vieira, P. Louro, M. Vieira, A. Fantoni, A. Steiger-Garção. IEEE sensor jornal, Vol. 12, NO. 6, (2012) pp. 1755-1762.
4. M.A. Vieira, M. Vieira, P. Louro, V. Silva, A., Applied Surface Science, DOI: 10.1016/j.apsusc.2013.01.020.
5. S. Randel, A.M.J. Koonen, S.C.J. Lee, F. Breyer, M. Garcia Larrode, J. Yang, A. Ng'Oma, G.J Rijckenberg, and H.P.A. Boom.. "ECOC 07 (Th 4.1.4). (pp. 1-4). Berlin, Germany, 2007.
6. M. Vieira, P. Louro, M. Fernandes, M. A. Vieira, A. Fantoni and J. Costa InTech, Chap.19, pp:403-425 (2011).
7. M. Vieira, A. Fantoni, P. Louro, M. Fernandes, R. Schwarz, G. Lavareda, and C. N. Carvalho, Vacuum, 82, Issue 12, 8 August 2008, pp: 1512-1516.
8. M. A. Vieira, M. Vieira, J. Costa, P. Louro, M. Fernandes, A. Fantoni, in Sensors & Transducers Journal Vol. 10, Special Issue, February 2011, pp.96-120.

 ISBN: 978-1-61208-297-4